Hindawi Publishing Corporation
Mathematical Problems in Engineering
Volume 2011, Article ID 397092, 18 pages
doi:10.1155/2011/397092

Research Article

Proportional-Derivative Observer-Based Backstepping Control for an Underwater Manipulator

M. Santhakumar[1, 2]

[1] *Ocean Robotics and Intelligence Lab, Division of Ocean Systems Engineering, School of Mechanical, Aerospace and Systems Engineering, Korean Advanced Institute of Science and Technology, Daejeon 305-701, Republic of Korea*
[2] *Robotics Research Lab, Department of Engineering Design, Indian Institute of Technology Madras, Chennai 600 036, India*

Correspondence should be addressed to M. Santhakumar, santha_radha@yahoo.co.in

Received 5 June 2011; Accepted 31 August 2011

Academic Editor: Xing-Gang Yan

Copyright © 2011 M. Santhakumar. This is an open access article distributed under the Creative Commons Attribution License, which permits unrestricted use, distribution, and reproduction in any medium, provided the original work is properly cited.

This paper investigates the performance of a new robust tracking control on the basis of proportional-derivative observer-based backstepping control applied on a three degrees of freedom underwater spatial manipulator. Hydrodynamic forces and moments such as added mass effects, damping effects, and restoring effects can be large and have a significant effect on the dynamic performance of the underwater manipulator. In this paper, a detailed closed-form dynamic model is derived using the recursive Newton-Euler algorithm, which extended to include the most significant hydrodynamic effects. In the dynamic modeling and simulation, the actuator and sensor dynamics of the system are also incorporated. The effectiveness of the proposed control scheme is demonstrated using numerical simulations along with comparative study between conventional proportional-integral-derivative (PID) controls. The results are confirmed that the actual states of joint trajectories of the underwater manipulator asymptotically follow the desired trajectories defined by the reference model even though the system is subjected to external disturbances and parameter uncertainties. Also, stability of the proposed (model reference control) control scheme is analyzed.

1. Introduction

The underwater manipulator has turned into a critical part/tool of underwater vehicles for performing deep-sea works such as opening and closing of valves, cutting, drilling, sampling, coring, and laying in the fields of scientific research and ocean systems engineering.

Autonomous manipulation, which is major focus of researches on manipulators mounted on underwater vehicles. Due to unstructured properties of deep-sea work, a good

understanding of the dynamics of a robotic manipulator mounted on a moving underwater vehicle is one of the important aspects of these kinds of deep-sea applications [1, 2].

During the last decade, most of the researches on underwater manipulator have focused and dedicated on the study of its dynamics and modeling, mechanical development, estimating parameters, and control schemes [1–7]. These manipulators are certainly different from the industrial and/or land-based manipulators; it is very demanding and difficult to control an underwater manipulator due to its nonlinear and time varying dynamics nature, variations in the hydrodynamic effects, external disturbances such as underwater current and waves. In addition to this, actuator and sensor characteristics, and their limitations make the controller design much more complicated. Therefore, the control scheme should be more robust and adaptive in nature. Several advanced control schemes have been proposed in the literature [8–15], either mounted on a movable and fixed platforms such as nonlinear feedback control, adaptive control, hybrid position and force control, coordinated motion control, model reference control, neural network-based control, and sliding mode control. In addition to this, most of the previous attempts have been made with planar manipulators. In order to make suitable control scheme for the manipulators, almost all the states are needed; however, as for the cost effectiveness and the reliability of the system, very few states only can be measured through sensors at the real time. The focus of this paper is on performance analysis of the underwater manipulator by considering all hydrodynamic effects and suggesting an effective scheme for controlling the manipulator motion which ensure the required performance in the presence of external disturbances and parameter variations. With the development of adaptive and robust backstepping designs in nonlinear systems, many fuzzy adaptive control schemes have been developed for unknown nonlinear systems not satisfying the matching conditions. Stable fuzzy adaptive backstepping controller design schemes were proposed for unknown nonlinear MIMO systems [16–19]. Though these control schemes had its own advantages over the other, in the real-time practice and applications, still traditional schemes such as PD, PI, PID schemes and sliding mode schemes are only used.

In this paper, a proportional-derivative observer-based backstepping control is proposed for a three degrees of freedom (dof) spatial underwater manipulator. One advantage of using this scheme is that the manipulator joint positions are only required from the real system (acquiring joint positions is a simple task and potentiometer can be used for this purpose), and the proposed system compensates all the nonlinearities in the system by introducing nonlinear elements in the input side, thus making the controller design more flexible. The manipulator states are estimated using this observer, which will be utilized by the controller. In this work, the dynamic model of the underwater manipulator is obtained using the iterative Newton-Euler method (it is extended from the basic scheme, which is applicable to the land based robots [20]) which includes all the hydrodynamic effects. The effectiveness of the proposed control scheme is confirmed with numerical simulations, and in the numerical study, the actuator and sensor characteristics such as time constant, efficiency, saturation limits, update rate, and sensor noises are considered. The Lyapunov analysis and its treatment on stability and robustness of the proposed scheme under parameter uncertainties are not explicitly dealt, which is left in this work for the scope of future work.

The reminder of this paper is organized as follows. The dynamic modeling of a 3 dof underwater manipulator is derived in Section 2. In Section 3, a nonlinear controller for the underwater manipulator based on observer-based backstepping control scheme is discussed. Detailed performance analysis of the underwater manipulator with different operating conditions is presented in Section 4. Finally, Section 5 holds the conclusions.

2. Modelling of the Underwater Manipulator

2.1. Kinematic Model of the Underwater Manipulator

The kinematic model of the underwater manipulator consists of two parts such as forward and inverse kinematics which are derived in this section as follows.

2.1.1. Forward Kinematics of the Underwater Manipulator

The mathematical relations of the end effector position/tool center point (TCP) or manipulator tip position with the known joint angles are derived here. The mathematical (kinematic) descriptions of the underwater manipulator are developed based on the Denavit-Hartenberg (D-H) parameters notation [20]. The establishment of the link coordinates system, as shown in Figure 2, yielded the D-H parameters shown in Table 1. On the basis of the underwater link parameters in Table 1, the homogeneous transformation matrix [20] is derived, that specifies the location of the end-effector or TCP with respect to the base coordinate system is expressed as

$$\mathbf{T}_4^0 = \begin{bmatrix} \mathbf{R}_4^0 & \mathbf{P}_4^0 \\ 0\ 0\ 0 & 1 \end{bmatrix} = \mathbf{T}_1^0\mathbf{T}_2^1\mathbf{T}_3^2\mathbf{T}_4^3,$$

$$\mathbf{T}_k^{k-1} = \begin{bmatrix} \cos\theta_k & -\sin\theta_k & 0 & a_{k-1} \\ \sin\theta_k\cos\alpha_{k-1} & \cos\theta_k\cos\alpha_{k-1} & -\sin\alpha_{k-1} & -\sin\alpha_{k-1}d_k \\ \sin\theta_k\sin\alpha_{k-1} & \cos\theta_k\sin\alpha_{k-1} & \cos\alpha_{k-1} & \cos\alpha_{k-1}d_k \\ 0 & 0 & 0 & 1 \end{bmatrix}. \tag{2.1}$$

The matrix $\mathbf{R}_4^0$ and the vector $\mathbf{P}_4^0 = [p_x\ \ p_y\ \ p_z]^T$ are the rotational matrix and the position vector from the base coordinates to the end-effector, respectively. p_x, p_y, and p_z are the manipulator tip positions on the x, y, and z axes, respectively. θ is the joint angle, α is the link offset or twist angle, d is the joint distance, and a is the link length.

From the above homogeneous transformation matrix, the end-effector's position for feedback control and the elements for solving Jacobian matrix can be obtained. On the basis of the experimental underwater manipulator parameters (refer to Table 1), the forward kinematic solutions are obtained and as given below:

$$\begin{aligned} p_x &= \cos\theta_1(L_1 + L_2\cos\theta_2 + L_3\cos(\theta_2+\theta_3)), \\ p_y &= \sin\theta_1(L_1 + L_2\cos\theta_2 + L_3\cos(\theta_2+\theta_3)), \\ p_z &= d_1 + L_2\sin\theta_2 + L_3\sin(\theta_2+\theta_3), \end{aligned} \tag{2.2}$$

where θ_1, θ_2, and θ_3 are the joint angles of the corresponding underwater manipulator links, respectively. L_1, L_2, and L_3 are the link lengths of the corresponding underwater manipulator links, respectively.

Table 1: D-H parameters of the 3dof underwater manipulator.

Joint axis (k)	Link offset (a_{k-1})	Link length (a_{k-1})	Joint distance (d_k)	Joint angle (θ_k)
1	0°	0	$d_1 = 0.1\,\text{m}$	θ_1
2	90°	$L_1 = 0.1\,\text{m}$	0	θ_2
3	0°	$L_2 = 0.4\,\text{m}$	0	θ_3
4	0°	$L_3 = 0.4\,\text{m}$	0	$\theta_4 = 0°$

2.1.2. Inverse Kinematics of the Underwater Manipulator

In the workspace-control system, each joint of the underwater manipulator is controlled by the joint angle command calculated from the differential inverse kinematics solutions on the basis of the known cartesian coordinates. The closed form inverse kinematic solutions of the 3dof underwater manipulator are described as

$$\begin{aligned} \theta_1 &= \operatorname{atan}2(p_y, p_x), \\ \theta_2 &= \operatorname{atan}2(ab - bc, ac + bd), \\ \theta_3 &= \operatorname{atan}2(\sin\theta_3, \cos\theta_3), \end{aligned} \tag{2.3}$$

where

$$\begin{aligned} \cos\theta_3 &= \frac{a^2 + b^2 - L_2^2 - L_3^2}{2L_2L_3}, \qquad \sin\theta_3 = \sqrt{1 - \cos^2\theta_3}, \\ a &= \frac{p_x}{\cos\theta_1} - L_1, \qquad b = p_z - d_1, \\ c &= L_3\cos\theta_3 + L_2, \qquad d = L_3\sin\theta_3. \end{aligned} \tag{2.4}$$

2.2. Dynamic Model of the Underwater Manipulator

The dynamic model of an underwater manipulator is developed through the recursive Newton-Euler algorithm. In this work, it is assumed that the underwater manipulator is buildup of cylindrical element. The effect of the hydrodynamic forces on circular cylindrical elements are described in the section, which mainly consist of added mass effects, frictional forces (such as linear skin friction, lift, and drag forces), munk moments (due to current loads), and buoyancy effects [21]. The force and moment interaction between two adjacent links are given below [20]:

$$\begin{aligned} {}^k\mathbf{f}_k &= \mathbf{R}_k^{k+1\,k+1}\mathbf{f}_{k+1} + \mathbf{F}_k - m_k\mathbf{g}_k + \mathbf{b}_k + \mathbf{p}_k, \\ {}^k\mathbf{t}_k &= \mathbf{R}_k^{k+1\,k+1}\mathbf{t}_{k+1} + \mathbf{d}_{k/k+1} \times \mathbf{R}_k^{k+1\,k+1}\mathbf{f}_{k+1} + \mathbf{d}_{k/kc} \times (\mathbf{F}_k - m_k\mathbf{g}_k + \mathbf{p}_k) + \mathbf{T}_k + \mathbf{d}_{k/kb} \times \mathbf{b}_k, \\ \mathbf{p}_k &= \mathbf{F}_{Lk} + \mathbf{F}_{Dk} + \mathbf{F}_{Sk}, \\ \mathbf{F}_{Sk} &= \mathbf{D}_s^{k\,k}\mathbf{v}_k\,, \\ \mathbf{F}_{Dk} &= \left|{}^k\mathbf{v}_k\right|^T \mathbf{D}_D^{k\,k}\mathbf{v}_k, \\ \mathbf{F}_{Lk} &= \left|{}^k\mathbf{v}_k\right|^T \mathbf{D}_D^{k\,k}\mathbf{v}_k, \end{aligned}$$

$$
\begin{aligned}
\mathbf{n}_k &= {}^k\mathbf{v}_k \times \left(\mathbf{M}_k^k \mathbf{v}_k\right),\\
\mathbf{F}_k &= \mathbf{M}_k\left({}^k\mathbf{a}_k + {}^k\boldsymbol{\alpha}_k \times {}^k\mathbf{d}_{k/kc} + {}^k\boldsymbol{\omega}_k \times \left({}^k\boldsymbol{\omega}_k \times {}^k\mathbf{d}_{k/kc}\right)\right),\\
\mathbf{T}_k &= \mathbf{I}_k\, {}^k\boldsymbol{\alpha}_k + {}^k\boldsymbol{\omega}_k \times \left(\mathbf{I}_k\, {}^k\boldsymbol{\omega}_k\right),\\
{}^{k+1}\boldsymbol{\omega}_{k+1} &= \mathbf{R}_{k+1}^k\, {}^k\boldsymbol{\omega}_k + \mathbf{z}^T \dot{q}_{k+1},\\
{}^{k+1}\boldsymbol{\alpha}_{k+1} &= \mathbf{R}_{k+1}^k\left({}^k\boldsymbol{\alpha}_k + {}^k\boldsymbol{\omega}_k \times \mathbf{z}^T q_k\right) + \mathbf{z}^T \ddot{q}_{k+1},\\
{}^{k+1}\mathbf{v}_{k+1} &= \mathbf{R}_{k+1}^k\, {}^k\mathbf{v}_k + {}^{k+1}\boldsymbol{\omega}_{k+1} \times {}^{k+1}\mathbf{d}_{k/kc},\\
{}^{k+1}\mathbf{a}_{k+1} &= \mathbf{R}_{k+1}^k\, {}^k\mathbf{a}_k + {}^{k+1}\boldsymbol{\alpha}_{k+1} \times {}^{k+1}\mathbf{d}_{k+1/k} + {}^{k+1}\boldsymbol{\omega}_{k+1} \times \left({}^{k+1}\boldsymbol{\omega}_{k+1} \times {}^{k+1}\mathbf{d}_{k+1/k}\right),\\
\mathbf{M}_k &= \begin{bmatrix} m_k + \dfrac{\pi\rho {r_k}^2 L_k}{10} & 0 & 0 \\ 0 & m_k + \pi\rho {r_k}^2 L_k & 0 \\ 0 & 0 & m_k + \pi\rho {r_k}^2 L_k \end{bmatrix},\\
\mathbf{I}_k &= \begin{bmatrix} I_x & 0 & 0 \\ 0 & I_y + \dfrac{\pi\rho {r_k}^2 {L_k}^3}{12} & 0 \\ 0 & 0 & I_z + \dfrac{\pi\rho {r_k}^2 {L_k}^3}{12} \end{bmatrix},
\end{aligned}
\tag{2.5}
$$

where $\mathbf{R}_k^{k+1}$ is the rotation matrix, $\mathbf{f}_k$ is the resultant force vector, $\mathbf{t}_k$ is the resultant moment vector, $\mathbf{p}_k$ is the linear and quadratic hydrodynamic friction forces, $\mathbf{F}_{Sk}$ is the linear skin friction force vector, $\mathbf{F}_{Dk}$ is the quadratic drag force vector, $\mathbf{F}_{Lk}$ is the quadratic lift force vector, $\mathbf{D}_S^k$ is the linear skin friction matrix, $\mathbf{D}_L^k$ is the diagonal matrix which contains lift coefficients, $\mathbf{D}_D^k$ is the diagonal matrix which contains drag coefficients, $\mathbf{g}_k$ is the gravity force vector, $\mathbf{b}_k$ is the buoyancy force vector, $\mathbf{n}_k$ is the hydrodynamic moment vector, $\mathbf{d}_{k/kb}$ is the vector from the center of buoyancy of the link, $\mathbf{d}_{k/kc}$ is the vector from the center of gravity of the link, $\mathbf{d}_{k/k+1}$ is the vector from joint k to $k+1$, $\mathbf{F}_k$ is the vector of total forces acting at the center of mass of link, $\mathbf{T}_k$ is the vector of total moments acting at the center of mass of link, $\mathbf{a}_k$ is the linear acceleration vector, $\boldsymbol{\alpha}_k$ is the angular acceleration vector, $\mathbf{v}_k$ is the linear velocity vector, $\boldsymbol{\omega}_k$ is the angular velocity vector, $\mathbf{m}_k$ is the mass of the link, $\mathbf{M}_k$ is the mass and added mass matrix of the link (located at the center of mass), and $\mathbf{I}_k$ is the moment of inertia and added moment of matrix of the link (located at the center of mass).

The joint torques of each axis is represented as

$$
\tau_{Rk} = \mathbf{z}^T\, {}^k\mathbf{t}_k, \tag{2.6}
$$

where $\mathbf{z}^T$ is the unit vector along the z-axis. The iterative Newton-Euler dynamics algorithm for all links symbolically yields the equations of motion for the underwater manipulator. The result of the equations of motion can be written as follows:

$$
\mathbf{M}_R(q)\ddot{\mathbf{q}} + \mathbf{C}_R(q,\dot{q})\dot{\mathbf{q}} + \mathbf{D}_R(q,\dot{q})\dot{\mathbf{q}} + \mathbf{g}_R(q) = \boldsymbol{\tau}_R, \tag{2.7}
$$

where $\mathbf{q}$ is the vector of joint variables, $\mathbf{q} = [\theta_1 \ \theta_2 \ \theta_3]^T$, $\theta_1, \theta_2, \theta_3$ are the joint angles of the corresponding underwater manipulator links, $\mathbf{M}_R(q)\ddot{\mathbf{q}}$ is the vector of inertial forces and moments of the manipulator, $\mathbf{C}_R(q,\dot{q})\dot{\mathbf{q}}$ is the vector of Coriolis and centripetal effects of the manipulator, $\mathbf{D}_R(q,\dot{q})\dot{\mathbf{q}}$ is the vector of damping effects of the manipulator, $\mathbf{g}_R(q)$ is the restoring vector of the manipulator, $\boldsymbol{\tau}_R = \boldsymbol{\tau}_{RC} + \boldsymbol{\tau}_{RO}$ is the input vector, $\boldsymbol{\tau}_{RC}$ is the control input vector, and $\boldsymbol{\tau}_{RO}$ is the observer input vector.

3. Observer-Based Backstepping Control

Our long-term objective is to develop a real-time, model-based, robust, and adaptive onboard nonlinear motion controller for an autonomous underwater vehicle-manipulator system (UVMS) to improve the manipulation autonomy so as to enable it to carry out complex intervention tasks involving energy transfer between the UVMS and the environment. Such a controller can overcome the issues associated with the parameter variations such as buoyancy variation, model uncertainties, disturbances, and noises. The first step in the development of such a real-time controller is the development of a model-based, robust, nonlinear controller for the underwater manipulator. In this paper, a novel nonlinear control technique is proposed and developed using the direct knowledge of reference manipulator dynamics through an observer. The robustness and performance of the proposed control technique are demonstrated with the help of numerical simulations. The details of controller development and simulation studies are presented below.

The dynamic model in (2.7) comprises nonlinear functions of state variables and characterizes the behaviour of the manipulator states. This feature of the dynamic model might lead us to believe that given any controller, the differential equation that models the control system in closed-loop should also be composed of nonlinear functions of the corresponding state variables. This perception applies to most of the conventional control laws. Nevertheless, there exists a controller which is nonlinear in the state variables but which leads to a closed-loop control system described by linear differential equations. In the following section, a novel observer-based backstepping control (refer to Proposition 3.1) which is capable of fulfilling the tracking control objective with proper selection of its design parameters is proposed.

Proposition 3.1. *Consider the system whose governing equations are given by* (2.7).

Let one defines a positive definite Lyapunov function as

$$V\left(\tilde{q},\dot{\tilde{q}},\tilde{q}_{\text{obs}},\dot{\tilde{q}}_{\text{obs}}\right) = \frac{1}{2}\left[\dot{\tilde{q}} + \varepsilon\tilde{q}\right]^{\mathbf{T}}\left[\dot{\tilde{q}} + \varepsilon\tilde{q}\right] + \frac{1}{2}\tilde{q}^T\left[\mathbf{K}_p + \varepsilon\mathbf{K}_D - \varepsilon^2\mathbf{I}\right]\tilde{q} + \frac{1}{2}\dot{\tilde{q}}_{\text{obs}}^T\mathbf{M}(\hat{q})\dot{\tilde{q}}_{\text{obs}} + \frac{1}{2}\tilde{q}_{\text{obs}}^T\mathbf{L}\tilde{q}_{\text{obs}} + \int_0^{\tilde{q}_{\text{obs}}}\mathbf{g}_{\tilde{q}_{\text{obs}}}^T(\varsigma)d\varsigma. \tag{3.1}$$

Choosing the control input vector and the observer input vector of the forms on the basis of backstepping control and proportional derivative schemes is given by

$$\boldsymbol{\tau}_{RC} = \mathbf{M}(\hat{q})\left(\ddot{q}_d + \mathbf{K}_p\tilde{q} + \mathbf{K}_D\dot{\tilde{q}}\right) + \mathbf{C}\left(\hat{q},\dot{\hat{q}}\right)\dot{\hat{q}} + \mathbf{D}\left(\hat{q},\dot{\hat{q}}\right)\dot{\hat{q}} + \mathbf{g}(\hat{q}),$$
$$\boldsymbol{\tau}_{RO} = -\mathbf{L}_D\dot{\tilde{q}}_{\text{obs}} - \mathbf{L}\tilde{q}_{\text{obs}} \tag{3.2}$$

will lead to the manipulator tracking (controller) and observer errors tending to zero asymptotically. That is the vehicle will follow the given desired trajectory.

Here, $\mathbf{L}$, $\mathbf{L}_D$, $\mathbf{K}_D$, *and* $\mathbf{K}_P$ *are symmetric positive definite (SPD) design matrices,* ε *is a positive constant, which satisfies* $\lambda_{\min}\{\mathbf{K}_D\} > \varepsilon > 0$, *and* $\lambda_{\min}$ *is the minimum Eigen value of the matrix* $\mathbf{K}_D$. $\tilde{q} = q_d - \hat{q}$ *denotes the vector of joint position errors of the estimated states,* $\tilde{\dot{q}} = \dot{q}_d - \hat{\dot{q}}$ *denotes the vector of joint velocity errors,* $\tilde{q}_{\text{obs}} = q - \hat{q}$ *denotes the vector of observer errors, and* $\tilde{\dot{q}}_{\text{obs}}$ *is the vector of observer error derivatives.* $\hat{q}$ *and* $\hat{\dot{q}}$ *are the vectors of estimated states of joint positions and velocities, respectively.* $q_d, \dot{q}_d$ *and* $\ddot{q}_d$, *are the vector of desired values of joint positions, velocities, and accelerations, respectively.*

Proof. The stability analysis of the closed-loop equation is analysed using Lyapunov's direct method [22].

Considering $\lambda_{\min}\{\mathbf{K}_D\} > \varepsilon > 0$, where $\mathbf{x} \in \Re^n$ is any nonzero vector, we obtain

$$\mathbf{x}^T \lambda_{\min}\{\mathbf{K}_D\}\mathbf{x} > \mathbf{x}^T \varepsilon \mathbf{x}. \tag{3.3}$$

Since $\mathbf{K}_D$ is by design a symmetric positive definite matrix,

$$\mathbf{x}^T(\mathbf{K}_D - \varepsilon\mathbf{I})\mathbf{x} > 0, \quad \forall \mathbf{x} \neq 0 \in \Re^n. \tag{3.4}$$

This means that the matrix $(\mathbf{K}_D - \varepsilon\mathbf{I})$ is symmetric positive definite; that is, $(\mathbf{K}_D - \varepsilon\mathbf{I}) > 0$. Considering all of this, the matrix $\mathbf{K}_P$ is symmetric positive definite and constant ε also positive by design; therefore,

$$\left(\mathbf{K}_P + \varepsilon\mathbf{K}_D - \varepsilon^2\mathbf{I}\right) > 0. \tag{3.5}$$

Matrices $\mathbf{M}(\hat{q})$ and $\mathbf{L}$ are positive definite by property [21] and by design, respectively, and the last term in the Lyapunov function is the potential energy of the system. Therefore, the candidate Lyapunov function is positive definite for all time. That is, $V(\tilde{q}, \tilde{\dot{q}}, \tilde{q}_{\text{obs}}, \tilde{\dot{q}}_{\text{obs}}) \geq 0$. However, for proving the asymptotically stable nature of the proposed system and errors convergence, the Lyapunov function $V(\tilde{q}, \tilde{\dot{q}}, \tilde{q}_{\text{obs}}, \tilde{\dot{q}}_{\text{obs}})$ is differentiated with respect to time along the state trajectories, and it yields

$$\begin{aligned}\dot{V}(\tilde{q}, \tilde{\dot{q}}, \tilde{q}_{\text{obs}}, \tilde{\dot{q}}_{\text{obs}}) = {} & \tilde{\dot{q}}^T \tilde{\ddot{q}} + \tilde{q}^T \left[\mathbf{K}_p + \varepsilon\mathbf{K}_D\right]\tilde{\dot{q}} + \tilde{\dot{q}}^T \varepsilon \tilde{\dot{q}} + \tilde{\dot{q}}^T \varepsilon \tilde{q} \\ & + \tilde{\dot{q}}_{\text{obs}}^T \left(\mathbf{M}(\hat{q})\tilde{\ddot{q}}_{\text{obs}} + \mathbf{L}\tilde{q}_{\text{obs}} + \mathbf{g}(\tilde{q}_{\text{obs}})\right) + \frac{1}{2}\tilde{\dot{q}}_{\text{obs}}^T \dot{\mathbf{M}}(\hat{q})\tilde{q}_{\text{obs}}.\end{aligned} \tag{3.6}$$

However, $\tilde{\ddot{\mathbf{q}}} = \ddot{\mathbf{q}}_d - \hat{\ddot{\mathbf{q}}}$, and $\hat{\ddot{\mathbf{q}}} = \mathbf{M}_R^{-1}(\hat{q})(\boldsymbol{\tau}_{RC} - \mathbf{C}(\hat{q}, \hat{\dot{q}})\hat{\dot{q}} - \mathbf{D}(\hat{q}, \hat{\dot{q}})\hat{\dot{q}} - \mathbf{g}(\hat{q}))$. Similarly, $\mathbf{M}_R(\hat{q})\tilde{\ddot{q}}_{\text{obs}} = \boldsymbol{\tau}_{RO} - (\mathbf{C}(\hat{q}, \hat{\dot{q}})\tilde{\dot{q}}_{\text{obs}} - \mathbf{D}(\hat{q}, \hat{\dot{q}})\tilde{\dot{q}}_{\text{obs}} - \mathbf{g}(\tilde{q}_{\text{obs}}))$, and $\tilde{\dot{q}}_{\text{obs}}^T(\dot{\mathbf{M}}(\hat{q}) - 2\mathbf{C}(\hat{q}, \hat{\dot{q}}))\tilde{\dot{q}}_{\text{obs}} = 0 \Rightarrow \dot{\mathbf{M}}(\hat{q}) = 2\mathbf{C}(\hat{q}, \hat{\dot{q}})$. Substituting $\tilde{\ddot{\mathbf{q}}}$, other above relations, the control and the observer vectors from (3.2) in (3.6), and simplifying the equation, it becomes

$$\begin{gathered}\dot{V}(\tilde{q}, \tilde{\dot{q}}, \tilde{q}_{\text{obs}}, \tilde{\dot{q}}_{\text{obs}}) = -\tilde{\dot{\mathbf{q}}}^T \left[\mathbf{K}_{DR} - \varepsilon\mathbf{I}\right]\tilde{\dot{\mathbf{q}}} - \varepsilon\tilde{\mathbf{q}}^T \mathbf{K}_{PR}\tilde{\mathbf{q}} - \tilde{\dot{q}}_{\text{obs}}^T \left(\mathbf{L}_{DR} + \mathbf{D}(\hat{q}, \hat{\dot{q}})\right)\tilde{\dot{q}}_{\text{obs}}, \\ \dot{V}(\tilde{q}, \tilde{\dot{q}}, \tilde{q}_{\text{obs}}, \tilde{\dot{q}}_{\text{obs}}) \leq 0.\end{gathered} \tag{3.7}$$

Since the matrices $\mathbf{L}_{DR}$, $(\mathbf{K}_D - \varepsilon\mathbf{I})$ and $\mathbf{K}_P$ are symmetric positive definite matrices by design, and $\mathbf{D}(\widehat{q}, \dot{\widehat{q}})$ damping matrix is positive definite by property [21], therefore, the function $\dot{V}(\tilde{q}, \dot{\tilde{q}}, \tilde{q}_{\text{obs}}, \dot{\tilde{q}}_{\text{obs}})$ in (3.7) is a negative definite function. From Lyapunov's stability theorem, the closed loop equation is uniformly asymptotically stable [22, 23], and therefore,

$$\begin{aligned} \lim_{t\to\infty} \dot{\tilde{\mathbf{q}}}(t) &= 0, \\ \lim_{t\to\infty} \tilde{\mathbf{q}}(t) &= 0. \end{aligned} \tag{3.8}$$

From (3.7), it can be observed that the tracking errors converge to zero asymptotically; however, $\dot{V}(\tilde{q}, \dot{\tilde{q}}, \tilde{q}_{\text{obs}}, \dot{\tilde{q}}_{\text{obs}}) = 0$ if and only if $\dot{\tilde{q}} = 0$, $\tilde{q} = 0$, and $\dot{\tilde{q}}_{\text{obs}} = 0$. From Barbalat's and modified LaSalle's lemmas [22, 23], it is necessary and sufficient that $\tilde{q} = 0$, $\dot{\tilde{q}} = 0$, and $\dot{\tilde{q}}_{\text{obs}} = 0$ for all time $(t \geq 0)$ [22]. Therefore, it must also hold that $\ddot{\tilde{q}}_{\text{obs}} = 0$ for all $t \geq 0$. Taking this into account, it can show from the closed loop equation that

$$0 = \mathbf{M}(\widehat{q})^{-1}\left(\mathbf{L}\tilde{q}_{\text{obs}} + \mathbf{g}\left(\tilde{q}_{\text{obs}}\right)\right). \tag{3.9}$$

Moreover, the observer gain matrix $\mathbf{L}$ is an SPD matrix by design and has been chosen in such a way that $\lambda_{\min}\{\mathbf{L}\} > \|\partial\mathbf{g}(\tilde{q}_{\text{obs}})/\partial\tilde{q}_{\text{obs}}\|$. Hence, $\tilde{q}_{\text{obs}} = 0$ for all $t \geq 0$ is its unique solution, and it can be observed that the observer errors also converge to zero asymptotically [22, 23]. That is,

$$\begin{aligned} \lim_{t\to\infty} \dot{\tilde{\mathbf{q}}}_{\text{obs}}(t) &= 0, \\ \lim_{t\to\infty} \tilde{\mathbf{q}}_{\text{obs}}(t) &= 0. \end{aligned} \tag{3.10}$$

□

Note 1. The proposed control scheme in (3.2) makes use of the knowledge of the system matrices $\mathbf{M}(\widehat{q}), \mathbf{C}(\widehat{q}, \dot{\widehat{q}})$, and $\mathbf{D}(\widehat{q}, \dot{\widehat{q}})$ and of the vector $\mathbf{g}(\widehat{q})$ for calculating the control input $\boldsymbol{\tau}_{RC}$ and hence referred to as model reference control (MRC) scheme. The block diagram that corresponds to the proposed controller is shown in Figure 2. The proposed Lyapunov analysis does not contain explicit treatment of the parametric uncertainties and external disturbance while taking temporal derivative along the closed-loop system trajectories.

4. Performance Analysis

4.1. Description of Tasks and the Underwater Manipulator

We have accomplished widespread computer-based numerical simulations to explore the tracking performance of the proposed observer-based backstepping control scheme. The manipulator used for this study consists of three dof spatial manipulator (refer Figure 1). The manipulator links are cylindrical in shape and the radii of links 1, 2, and 3 are 0.1 m, 0.1 m, and 0.1 m, respectively. The lengths of link 1, 2, and 3 are 0.1 m, 0.4 m, and 0.4 m, respectively. The link masses (along with oil conserved motors) are 3.15 kg, 15.67 kg, and 15.67 kg, respectively. Here, the links are considered as cylindrical shape, because such shape provides uniform hydrodynamic reactions and is one of the primary candidates for possible link

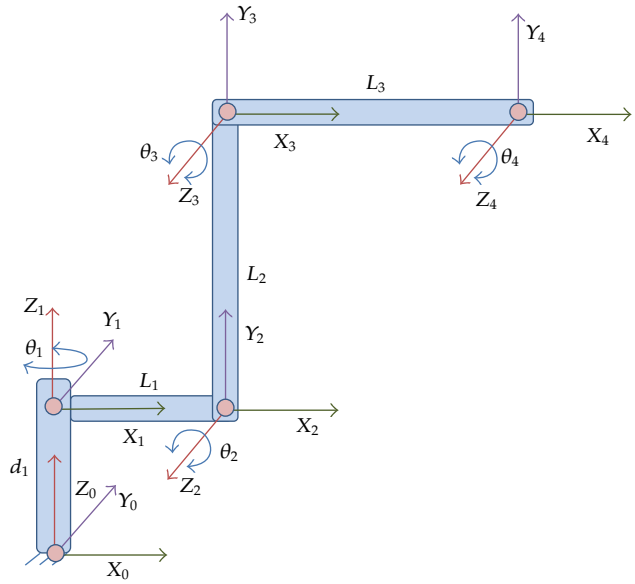

Figure 1: Establishing link coordinate systems of the manipulator.

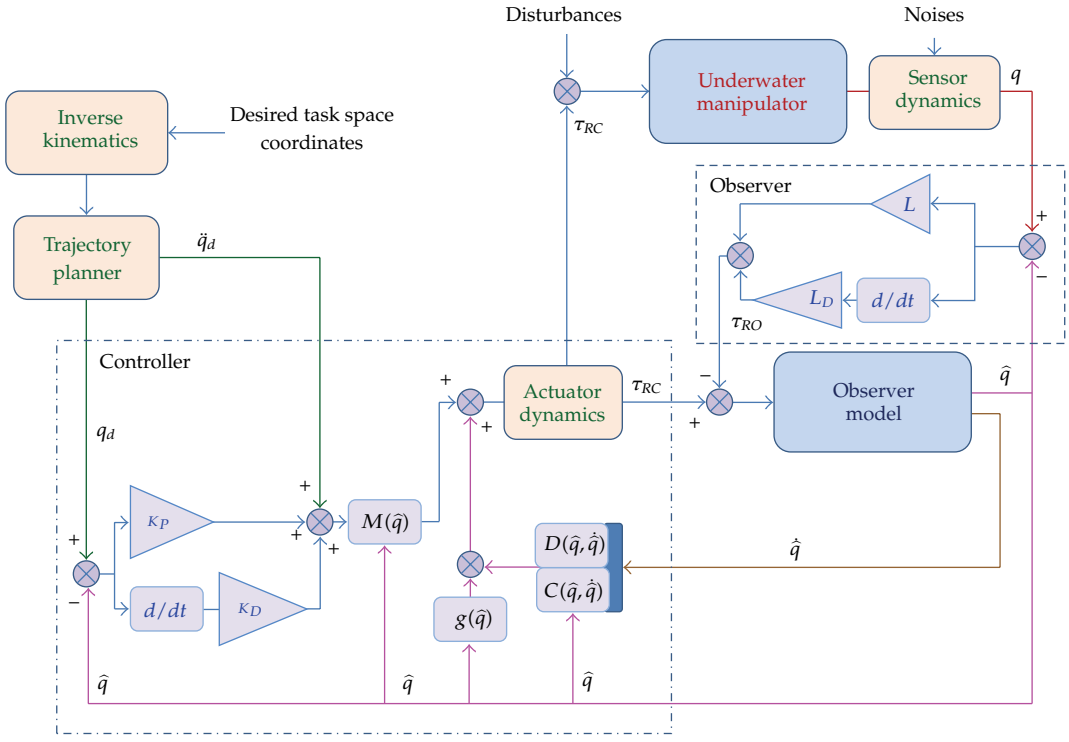

Figure 2: Block diagram of proposed control scheme for an underwater manipulator.

geometry for underwater manipulators. Although it is cylindrical, our mathematical framework does not depend on any particular shapes, and it can be easily accommodated in any other shapes. Indeed, cylindrical underwater manipulators are available in the present market [24].

Hydrodynamic parameters of the manipulator were estimated using empirical relations based on strip theory. This method is verified using available literature; therefore, these values are reliable and can be used for further developments. Some parameters like inertia, centre of gravity, and centre of buoyancy are calculated from the geometrical design of the manipulator. We have compared our results with that of traditional PID controller, and the following control vector is considered for the manipulator and given by

$$\boldsymbol{\tau}_{RC} = \mathbf{K}_D\dot{\tilde{\mathbf{q}}} + \mathbf{K}_P\tilde{\mathbf{q}} + \mathbf{K}_I\int \tilde{\mathbf{q}}\,dt, \tag{4.1}$$

where, $\mathbf{K}_P$, $\mathbf{K}_{\mathrm{I}}$, and $\mathbf{K}_D$ are the proportional, integral, and derivative gain matrices.

There are two basic trajectories that have been considered for the simulations, a straight line trajectory with a length of 0.52 m and a circular trajectory with a diameter of 0.4 m in 3D space. This is for the reason that most of the underwater intervention tasks involved these types of trajectories and any spatial trajectory can be arranged by combining these trajectories. In the performance analysis, the sensory noises in joint position measurements are considered as Gaussian noise of 0.01 rad mean and 0.01 rad standard deviation for the joint position measurements. The actuator characteristics also incorporated in the simulations. All the actuators are considered as an identical one, and the following actuator characteristics are considered for the analysis: the response delay time is 200 ms, efficiency is 95%, and saturation limits of the actuators are ±5 Nm. The controller update rate and sensor response time are considered as 100 ms each.

4.2. Results and Discussions

The controller gain values for both proposed MRC and traditional PID schemes are tuned based on a combined Taguchi's method and genetic algorithms (GA) with the minimization of integral squared error (ISE) as the cost/objective function [25, 26], and here, we have considered both proposed and PID control performances are almost equal in the ideal situation, which makes the controller performance comparison quite reasonable for the further analysis and gives much better way of understanding between these controller performances. The combined Taguchi's method and GA scheme makes tuning the controller parameters much more simple and effective. In this method, the initial step is to finding the limits of controller gain values for GA tuning scheme, which obtained through Taguchi's method. It makes the GA performance with less iterations and faster convergence. The controllers parameters are obtained through this method are given in Table 2. The same set of controller parameters are used throughout the entire performance analysis. The observer settings are common for both controllers and these values tuned through the above method and are given in Table 2.

In the initial set of simulations, only nonzero initial errors have considered, and all other conditions are considered as an ideal one, that is, the observer model exactly equivalent to the system, no external disturbances, and no sensor noises. The manipulator commanded to track a straight-line trajectory in the 3D space about a length of 0.52 m, from (0.2, 0.6, 0.5) m to (0.5, 0.3, 0.2) m with the time span of 10 s. The manipulator initial position errors in task

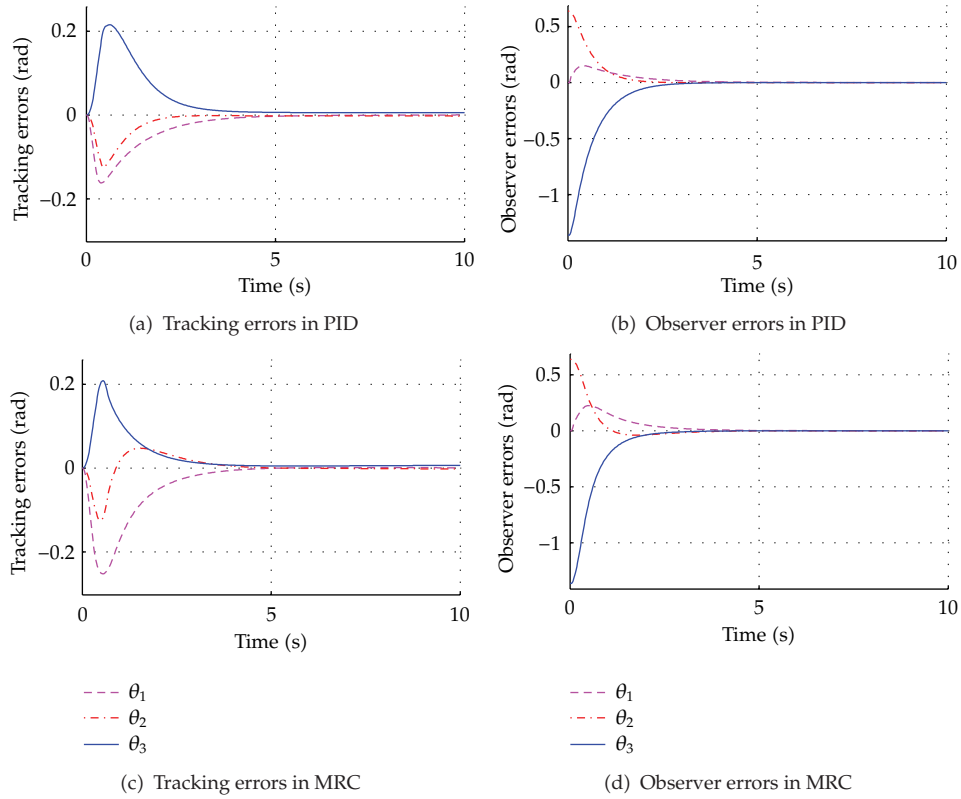

(a) Tracking errors in PID

(b) Observer errors in PID

(c) Tracking errors in MRC

(d) Observer errors in MRC

Figure 3: Time trajectories of the joint position errors for the straight line trajectory in an ideal condition.

Table 2: Controller parameter settings for simulations.

PID controller parameters	Values	Proposed controller parameters	Values
K_P	diag(60, 80, 75)	K_{PR}	diag(5, 10, 12)
K_D	diag(35, 40, 50)	K_{DR}	diag(3, 5, 8)
K_I	diag(1, 1.5, 2)		
PD observer parameters			
L	diag(10, 16, 18)	L_{DR}	diag(8, 10, 11)

space (x, y, and z) are 0.1 m, 0.3 m, and 0.25 m, respectively. Both the controller performances are presented in Figures 3 to 5. Figure 3 shows the time trajectories of tracking and observer errors of the joint positions, Figure 4 shows the time histories of tracking and observer errors of the manipulator task space coordinates, and Figure 5 shows the 3D space desired and actual task space trajectories. From the results, it is observed that both the controllers are working almost similar fashion and produced satisfactory results. In a deeper observation, it shows that the PID controller performance little far better than the proposed controller. This is mainly to make fair comparison between these two controllers in the presence of external disturbances, parameter uncertainties, and sensor noises and illustrate the effectiveness of the proposed controller.

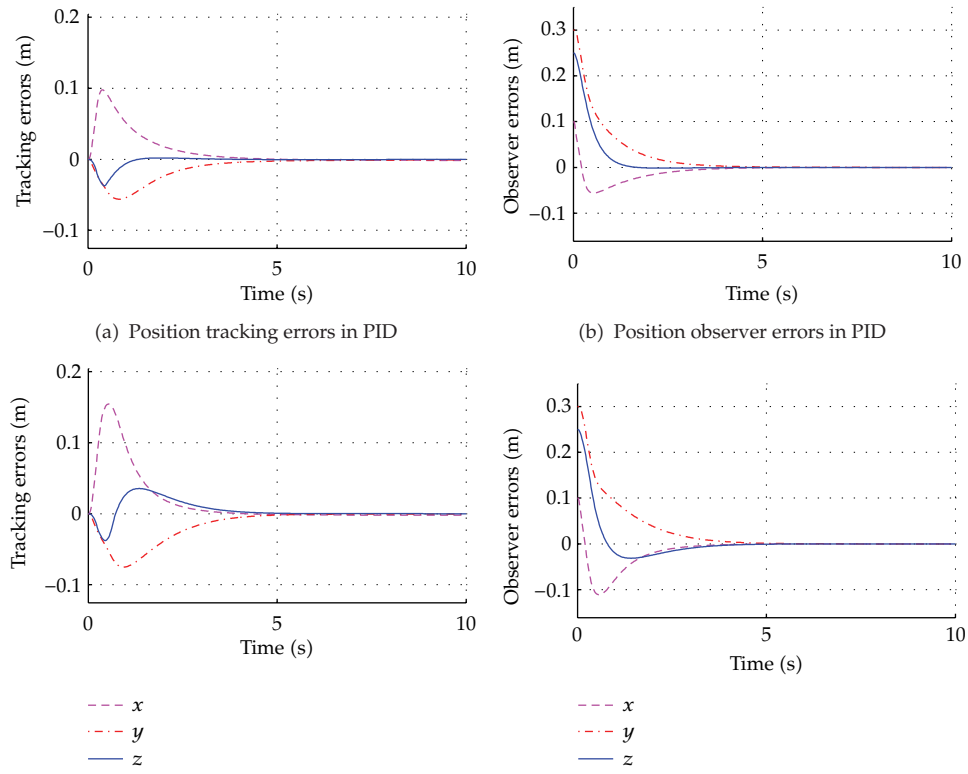

(a) Position tracking errors in PID

(b) Position observer errors in PID

(c) Position tracking errors in MRC

(d) Position observer errors in MRC

Figure 4: Time trajectories of the task space (xyz) errors for the straight line trajectory in an ideal condition.

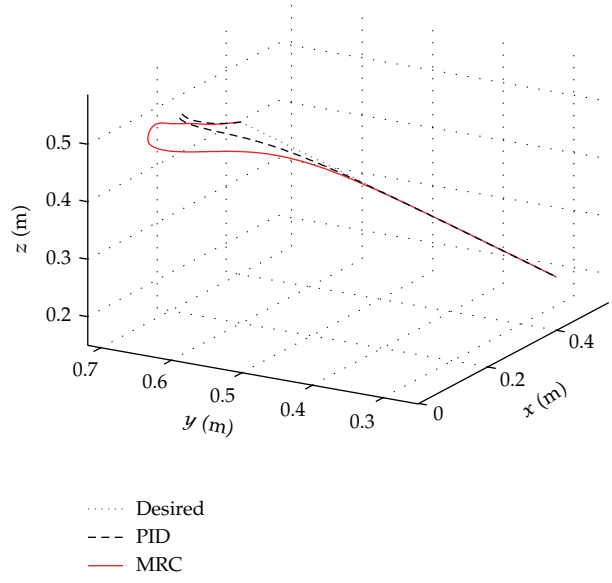

Figure 5: Task space (xyz) trajectories for the straight line trajectory in an ideal condition.

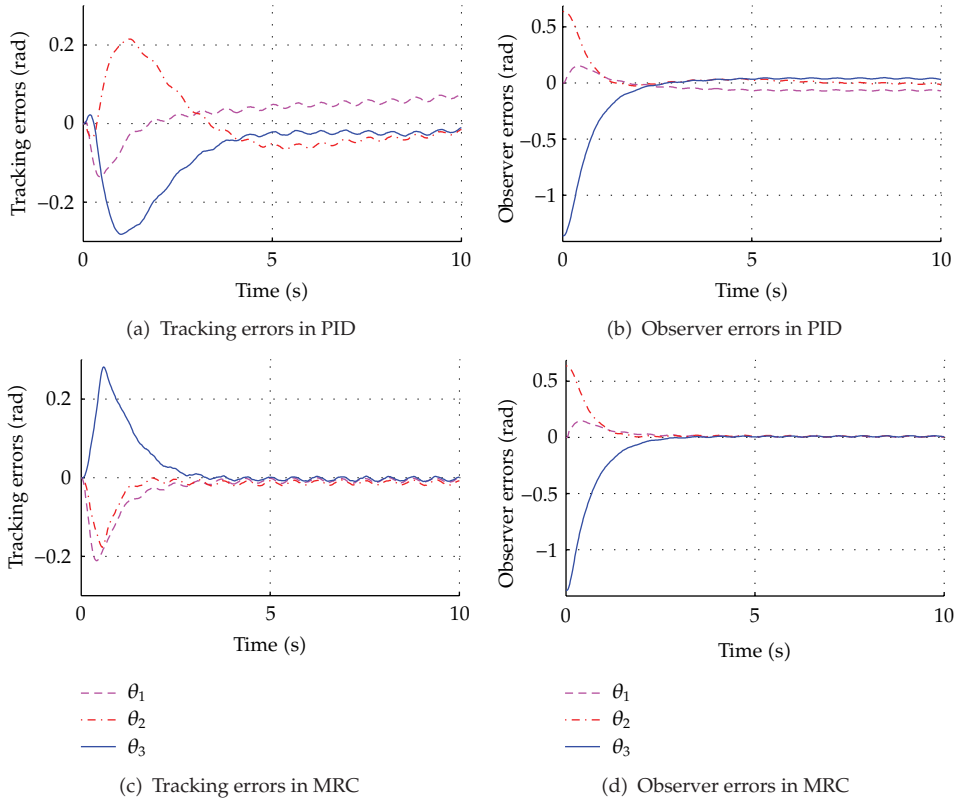

(a) Tracking errors in PID

(b) Observer errors in PID

(c) Tracking errors in MRC

(d) Observer errors in MRC

Figure 6: Time trajectories of the joint position errors for the straight line trajectory in an uncertain and disturbed condition.

In order to demonstrate the adaptability and robustness of the proposed controller, an uncertain condition is considered for the simulations, where the manipulator parameters are assumed to be 10% of uncertainties, a payload of 10 kg is considered, and the manipulator tracking the given desired task space trajectories in the presence of an unknown underwater current (with an average current speed of 0.5 m/s, side slip and angle of attack are 45° each) and the sensory noises in joint position measurements are considered as Gaussian noise of 0.01 rad mean and 0.01 rad standard deviation. The simulation results for both straight line and circular trajectories in the presence of disturbances and uncertainties are presented in Figures 6, 7, 8, 9, 10, and 11, and from these results, it is observed that the proposed observer-based backstepping controller is good in adapting the uncertainties and external disturbances (refer to task space trajectories in Figures 8 and 11). In both trajectory tracking cases, the manipulator actuator torques are not exceeding ±1 Nm (except initial stage, because during this stage the nonzero initial errors are compensated; therefore, in the initial stage, the actuator reaches its saturation limits ±5 Nm), which are well with the range of actuators.

In this work, we have provided numerical simulation results to investigate the performance and to demonstrate the effectiveness of the proposed control scheme. These results are intuitive, promising, and point out the prospective of the proposed approach. Therefore, this work can be extended to autonomous underwater vehicle-manipulator system, and it can also be extended to develop a coordinated control scheme for the same. On the other hand,

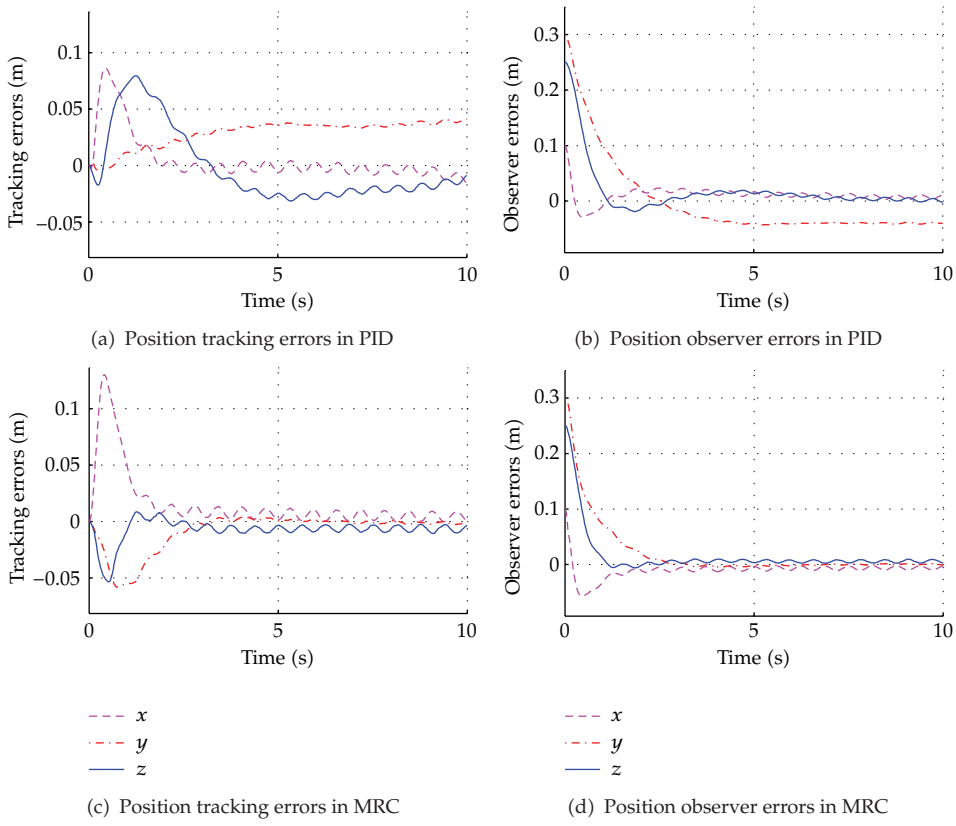

(a) Position tracking errors in PID

(b) Position observer errors in PID

(c) Position tracking errors in MRC

(d) Position observer errors in MRC

Figure 7: Time trajectories of the task space (xyz) errors for the straight line trajectory in an uncertain and disturbed condition.

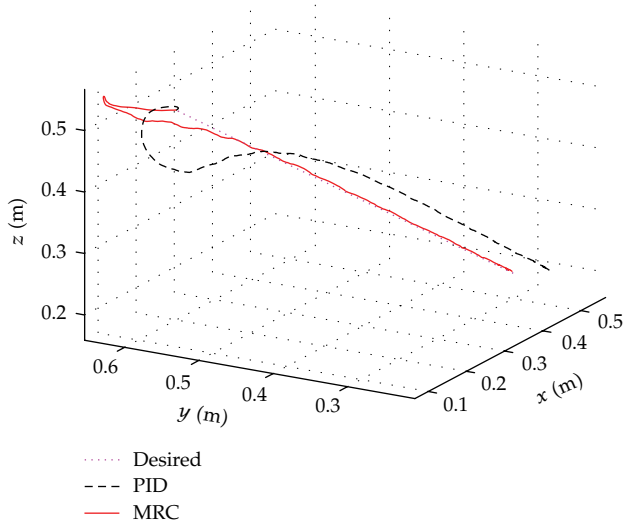

Figure 8: Task space (xyz) trajectories for the straight line trajectory in an uncertain and disturbed condition.

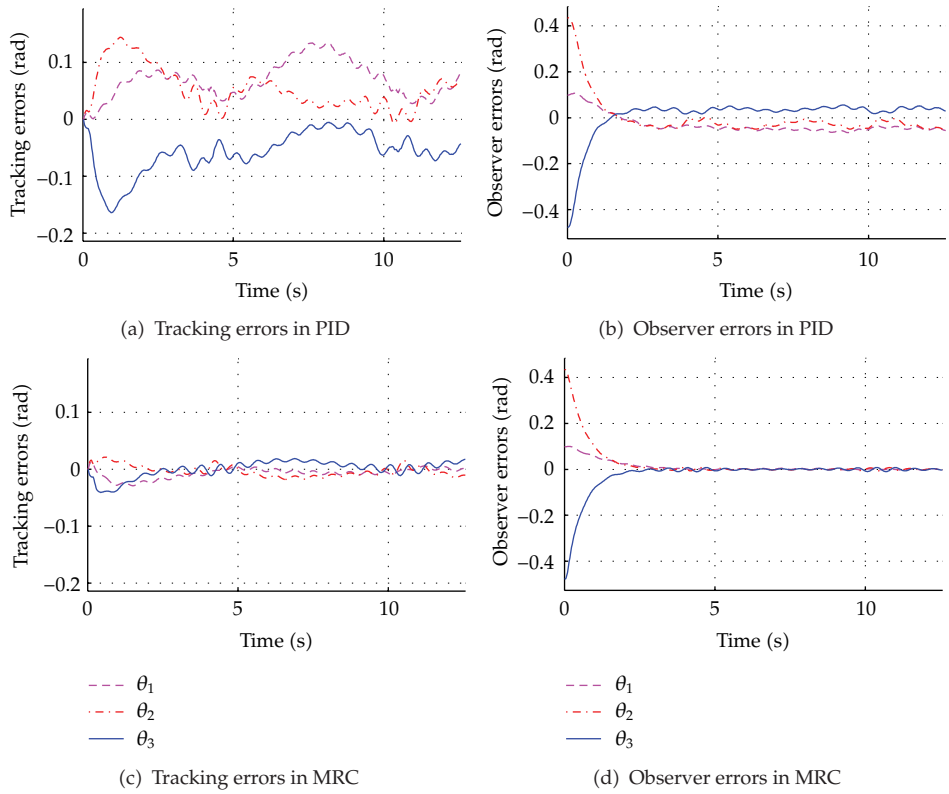

(a) Tracking errors in PID

(b) Observer errors in PID

(c) Tracking errors in MRC

(d) Observer errors in MRC

Figure 9: Time trajectories of the joint position errors for the circular trajectory in an uncertain and disturbed condition.

these results are based on numerical simulations; therefore, it is important that extensive real-time experiments need to be conducted to validate the advantages of the proposed scheme which will be available in near future.

5. Conclusion

The tracking performance of the proportional-derivate observer-based backstepping controlled spatial underwater manipulator is investigated. The simulation results demonstrate that the actual joint trajectories asymptotically follow the desired trajectories defined by the reference observer model. Despite the effects of hydrodynamics on the manipulator, parameter uncertainties, and external disturbances (underwater current), the tracking performance of the proposed control scheme produced better performance and is also confirmed to be good and satisfactory. The proposed proportional-derivative observer has shown its importance to estimating the state variables, and in this work, we have considered only the joint positions (i.e., only corresponding potentiometer outputs) which is cost effective. The values of proposed controller and PID controller gains are tuned on the basis of combined Taguchi's method and genetic algorithms. It is worth to design such scheme to obtain optimal values which probably improves the controller performance. The proposed scheme effectiveness has been demonstrated only with computer simulations, whereas this is an important first step

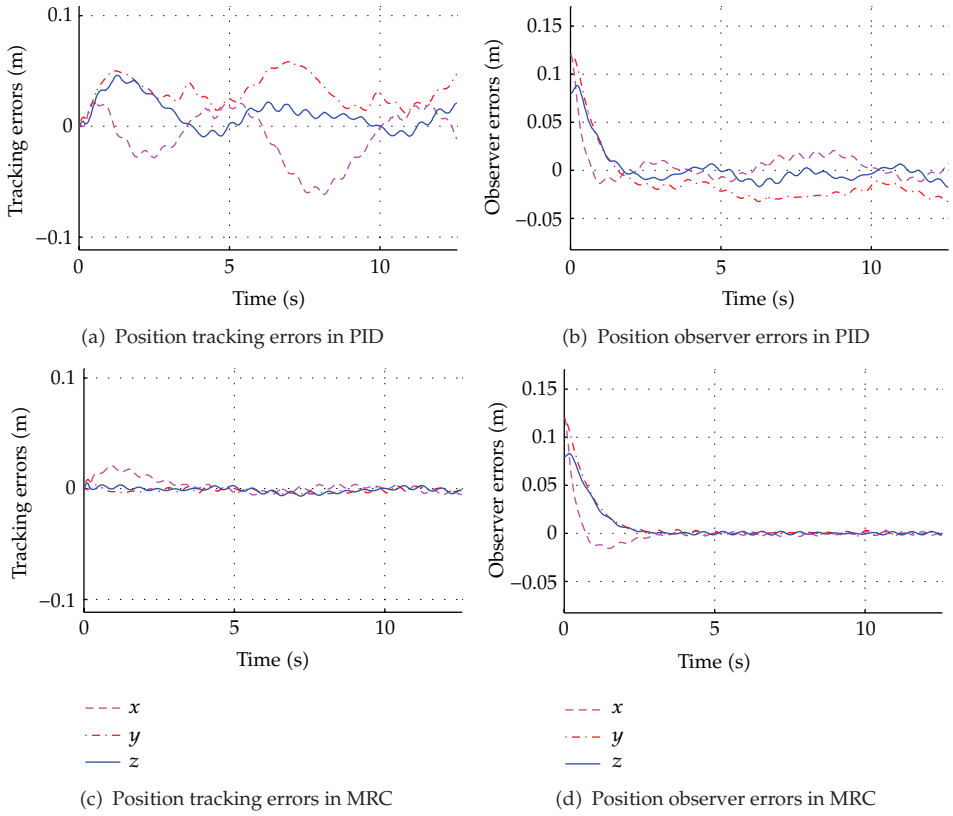

(a) Position tracking errors in PID

(b) Position observer errors in PID

(c) Position tracking errors in MRC

(d) Position observer errors in MRC

Figure 10: Time trajectories of the task space (xyz) errors for the circular trajectory in an uncertain and disturbed condition.

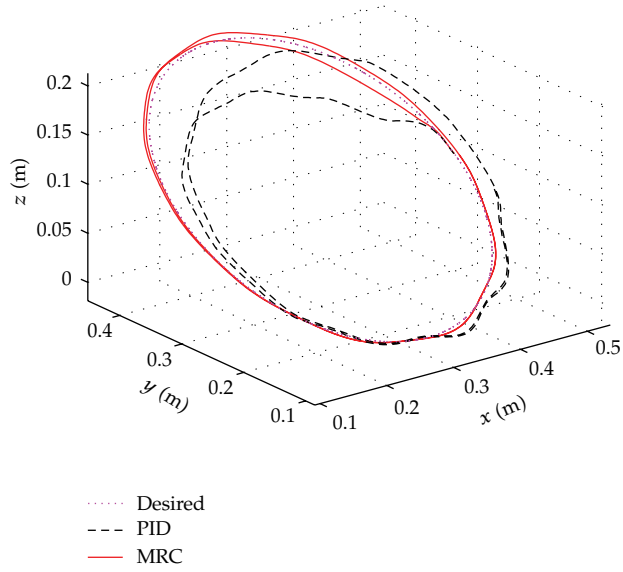

Figure 11: Task space (xyz) trajectories for the circular trajectory in an uncertain and disturbed condition.

before preceding the actual real-time experiments in order to understand the challenges associated with the system. Therefore, as a future work, the proposed scheme can be validated through real-time experiments. The Lyapunov analysis does not contain any explicit treatment of the parametric uncertainties and external disturbance while taking temporal derivative along the closed-loop system trajectories. Therefore, as a future work, the proposed scheme stability and its robustness can be proved in the presence of parametric uncertainties and external disturbances in near future.

Acknowledgments

The author would like to acknowledge Professor Jinwhan Kim for his valuable suggestions and discussions on underwater manipulator. This research was supported in part by the WCU (World Class University) program through the National Research Foundation of Korea funded by the Ministry of Education, Science and, Technology (R31-2008-000-10045-0).

References

[1] G. Antonelli, F. Caccavale, S. Chiaverini, and L. Villani, "Tracking control for underwater vehicle-manipulator systems with velocity estimation," *IEEE Journal of Oceanic Engineering*, vol. 25, no. 3, pp. 399–413, 2000.

[2] G. Marani, S. K. Choi, and J. Yuh, "Underwater autonomous manipulation for intervention missions AUVs," *Ocean Engineering*, vol. 36, no. 1, pp. 15–23, 2009.

[3] McMillan, R. McGhee, and D. Orin, "Efficient dynamic simulation of an underwater vehicle with a robotic manipulator," *IEEE Transactions on Systems, Man and Cybernetics*, vol. 25, no. 8, pp. 1194–1206, 1995.

[4] L. Benoit and J. R. Marc, "Dynamic analysis of a manipulator in a fluid environment," *International Journal of Robotics Research*, vol. 13, no. 3, pp. 221–231, 1994.

[5] T. J. Tarn, G. A. Shoults, and S. P. Yang, "A dynamic model of an underwater vehicle with a robotic manipulator using Kane's method," *Autonomous Robots*, vol. 3, no. 2-3, pp. 269–283, 1996.

[6] H. Mahesh, J. Yuh, and R. Lakshmi, "Coordinated control of an underwater vehicle and robotic manipulator," *Journal of Robotic Systems*, vol. 8, no. 3, pp. 339–370, 1991.

[7] K. Ioi and K. Itoh, "Modelling and simulation of an underwater manipulator," *Advanced Robotics*, vol. 4, no. 4, pp. 303–317, 1989.

[8] N. Sarkar and T. K. Podder, "Coordinated motion planning and control of autonomous underwater vehicle-manipulator systems subject to drag optimization," *IEEE Journal of Oceanic Engineering*, vol. 26, no. 2, pp. 228–239, 2001.

[9] T. W. McLain, S. M. Rock, and M. J. Lee, "Experiments in the coordinated control of an underwater arm/vehicle system," *Autonomous Robots*, vol. 3, no. 2-3, pp. 213–232, 1996.

[10] B. H. Jun, P. M. Lee, and J. Lee, "Manipulability analysis of underwater robotic arms on ROV and application to task-oriented joint configuration," in *Proceedings of the Oceans MTS/ IEEE and Techno Ocean (OTO '04)*, pp. 1548–1553, Kobe, Japan, 2004.

[11] P. M. Lee, H. J. Bong, W. H. Seok, and K. L. Yong, "System design of an ROV with manipulators and adaptive control of it," in *Proceedings of the International Symposium on Underwater Technology (UT '00)*, pp. 431–436, Tokyo, Japan, 2000.

[12] D. M. Lane, M. W. Dunnigan, A. C. Clegg, P. Dauchez, and L. Cellier, "A comparison between robust and adaptive hybrid position/force control schemes for hydraulic underwater manipulators," *Transactions of the Institute of Measurement and Control*, vol. 19, no. 2, pp. 107–116, 1997.

[13] X. Guohua, Z. Ying, and X. Xianbo, "Trajectory tracking for underwater manipulator using sliding mode control," in *Proceedings of the IEEE International Conference on Robotics and Biomimetics (ROBIO '07)*, pp. 2127–2132, 2007.

[14] S. R. Pandian and N. A. Sakagami, "A neuro-fuzzy controller for underwater robot manipulators," in *Proceedings of the 11th International Conference on Control Automation Robotics and Vision (ICARCV '10)*, pp. 2135–2140, Singapore, 2010.

[15] M. Lee and H.-S. Choi, "A robust neural controller for underwater robot manipulators," *IEEE Transactions on Neural Networks*, vol. 11, no. 6, pp. 1465–1470, 2000.
[16] S. Tong and Y. Li, "Observer-based fuzzy adaptive control for strict-feedback nonlinear systems," *Fuzzy Sets and Systems*, vol. 160, no. 12, pp. 1749–1764, 2009.
[17] T. Shaocheng, C. Li, and Y. Li, "Fuzzy adaptive observer backstepping control for MIMO nonlinear systems," *Fuzzy Sets and Systems*, vol. 160, no. 19, pp. 2755–2775, 2009.
[18] T. Shaocheng, C. Bin, and W. Yongfu, "Fuzzy adaptive output feedback control for MIMO nonlinear systems," *Fuzzy Sets and Systems*, vol. 156, no. 2, pp. 285–299, 2005.
[19] T. Shaocheng, X.-L. He, and H.-G. Zhang, "A combined backstepping and small-gain approach to robust adaptive fuzzy output feedback control," *IEEE Transactions on Fuzzy Systems*, vol. 17, no. 5, pp. 1059–1069, 2009.
[20] J. J. Craig, *Introduction to Robotics: Mechanics and Control*, Addison Wesley, Boston, Mass, USA, 1986.
[21] T. I. Fossen, *Guidance and Control of Ocean Vehicles*, Wiley, Chichester, UK, 1994.
[22] J. J. E. Slotine and W. Li, *Applied Nonlinear Control*, Prentice-Hall, Englewood Cliffs, NJ, USA, 1991.
[23] H. K. Khalil, *Nonlinear Systems*, Prentice Hall, New York, NY, USA, 2002.
[24] Ansaldo Nucleare, *Underwater Manipulator MARIS 7080 Use and Maintenance Manual*, Ansaldo Nuclear Division, Genoa, Italy, 1996.
[25] K. Deb, *Optimization for Engineering Design: Algorithms and Examples*, Prentice Hall, India, 2004.
[26] M. Santhakumar and T. Asokan, "Application of robust design techniques for underwater vehicle control," in *Proceedings of the ISOPE OMS-2009: 8th ISOPE Ocean Mining Symposium*, pp. 285–289, Chennai, India, 2009.

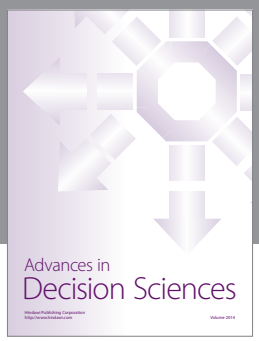

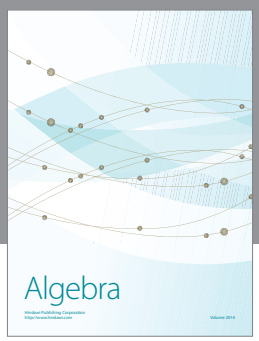

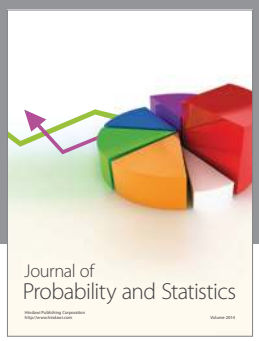

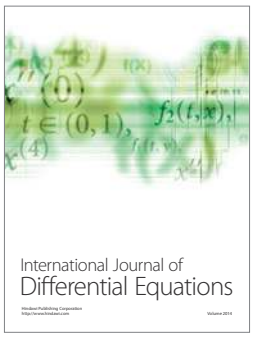

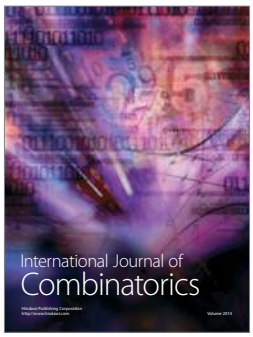

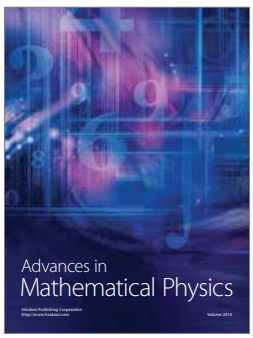

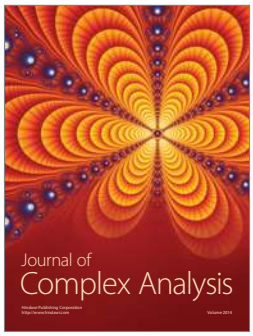

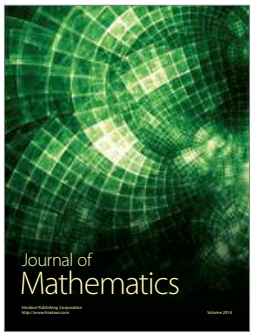

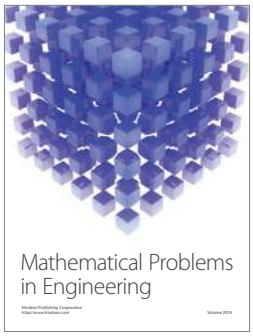

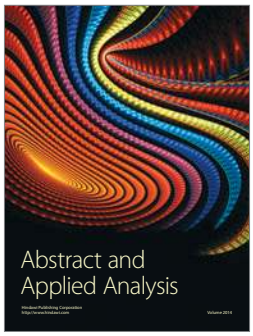

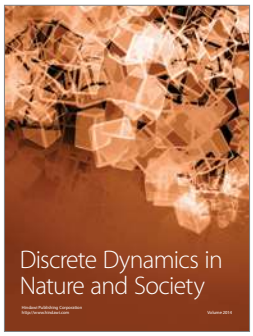

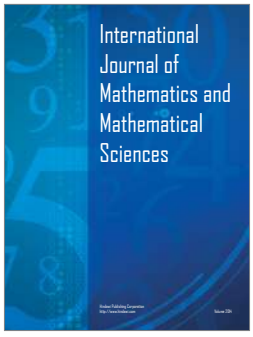

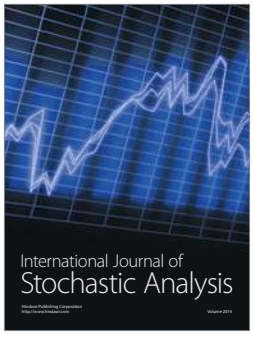

Hindawi
Submit your manuscripts at
http://www.hindawi.com